The Galactic Globular Cluster M5 (NGC 5904) as a Particle Physics Laboratory: The axion-electron coupling case

Nicolás Viaux M.

Pontificia Universidad Católica de Chile (PUC)

Collaborators: Márcio Catelan (PUC), Raffelt ,G. (MPP), Redondo ,J. (MPP), Stetson ,P. (DAO), Valcarce A.A (UFRN)

PATRAS 2013

This constraint was done before (Raffelt & Weiss 1995 based in Raffelt 1990) why do it again?

- Now we have new and precise observations.
- Updated stellar evolution code.

This constraint was done before (Raffelt & Weiss 1995 based in Raffelt 1990) why do it again?

- IAXO will contraint g_{aee} so a deep analysis on the uncertainties is needed to provide C.L.

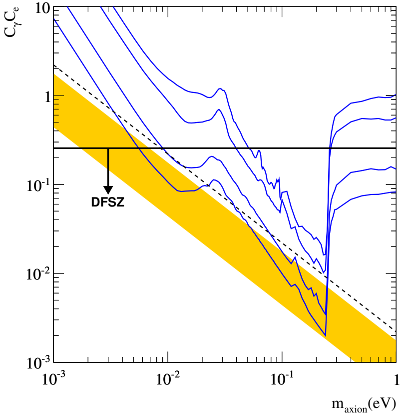

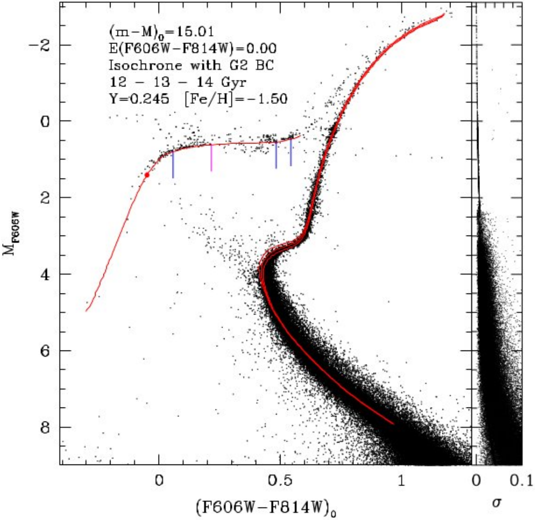

Figure: CMD of M3, A.A Valcarce PhD Thesis (2011)

Stellar evolution

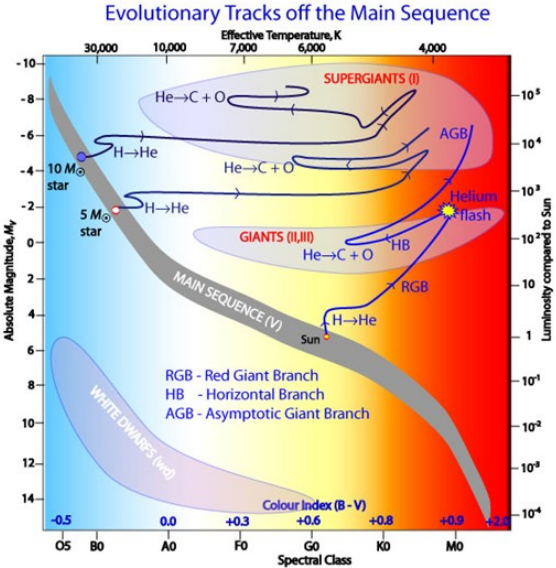

So, including new weakly interacting particle like axion, will drain energy from the star that escape easily, then modifying the route of the star in his evolution. Comparing this new route with observation, is possible to constraint g_{aee}.

$$\mathcal{L}_{int} = \frac{C_j}{2f_a}\overline{\Psi}_j\gamma^\mu\Psi_j\partial_\mu a \tag{1}$$

For axion-electron interaction,

$$g_{aee} = C_e m_e/f_a \tag{2}$$

and

$$C_e = \frac{\cos^2\beta}{3} \tag{3}$$

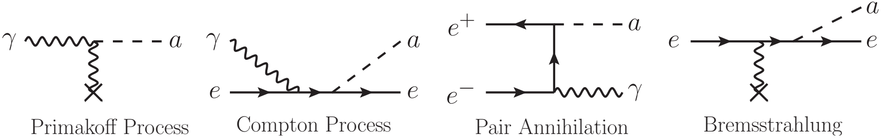

Figure: Thermal axion emission processes in normal stars (Raffelt 2012, `http://arxiv.org/abs/1201.1637`)

Axion emission processes in a non nuclear medium

Compton emission

One simple way to produce axions is in the Compton process $\gamma + e \rightarrow e + a$, where the energy-loss rate is (Raffelt & Weiss 1995):

$$\epsilon_C = 33.0 \cdot \left(\frac{g_{aee}^2}{4\pi \times 10^{-26}} \right) \cdot Y_e \cdot T_8^6 \cdot F[erg/g/s] \tag{4}$$

where $T_8 = T/10^8, Y_e = n_e m_u/\rho$ is the electron per baryon number, $n_e = (\rho/m_u) \sum_j X_j Z_j / A_j$ is the electron density, m_u is the atomic mass unit, X_j is the mass fraction of the j element, A_j is the atomic mass and $Z_j e$ is the charge. F account for relativistic and degenerate effects.

Axion emission processes in a non nuclear medium

Nondegenerate Bremsstrahlung

Another process that create axions in non-degenerate conditions is the non-degenerate bremsstrahlung: $e + (Z, A) \rightarrow (Z, A) + a$ and $e + e \rightarrow e + e + a$. This emission rate is provided by Raffelt & Weiss 1995 but only for a composition of Hydrogen and Helium. Now we want to include metals, the formula (8) of Raffelt & Weiss 1995 becomes (Raffelt 1996):

$$\epsilon_{ND} = 590.0 \cdot \left(\frac{g_{aee}^2}{4\pi \times 10^{-26}} \right) \cdot T_8^{2.5} \cdot \rho_6 \sum_j \left(\frac{X_j Z_j}{A_j} \right) \sum_j \frac{X_j}{A_j} \left(Z_j^2 + \frac{Z_j}{\sqrt{2}} \right) \tag{5}$$

$[erg/g/s]$
where $\rho_6 = \rho/10^6$.

Axion emission processes in a non nuclear medium

Degenerate Bremsstrahlung

(Raffelt 1996):

$$\epsilon_D = 10.8 \cdot \left(\frac{g_{aee}^2}{4\pi \times 10^{-26}} \right) \left(\sum_j \frac{X_j Z_j^2}{A_j} \right) \cdot T_8^4 \cdot F[erg/g/s] \quad (6)$$

where

$$F = \frac{2}{3} \ln \left(\frac{2+\kappa^2}{\kappa^2} \right) + \left[\frac{2+5\kappa^2}{15} \ln \left(\frac{2+\kappa^2}{\kappa^2} \right) - \frac{2}{3} \right] \beta_F^2 + \mathcal{O}(\beta_F^4) \quad (7)$$

$(\beta_F = p_F/E_F)$

And

$$\kappa^2 = \frac{\kappa_D^2}{2p_F^2} = \frac{4\pi\alpha \sum_j Z_j n_j}{T} \frac{1}{2p_F^2} \quad (8)$$

Axion emission trough all the star (RGB star)

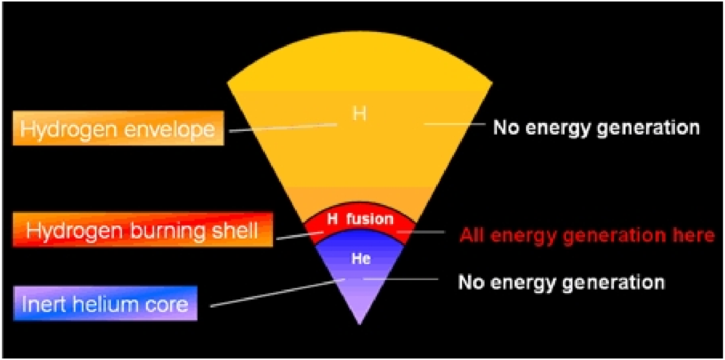

(Raffelt & Weiss 1995):

$$\epsilon_T = (\epsilon_{ND}^{-1} + \epsilon_D^{-1})^{-1} + \epsilon_C \quad (9)$$

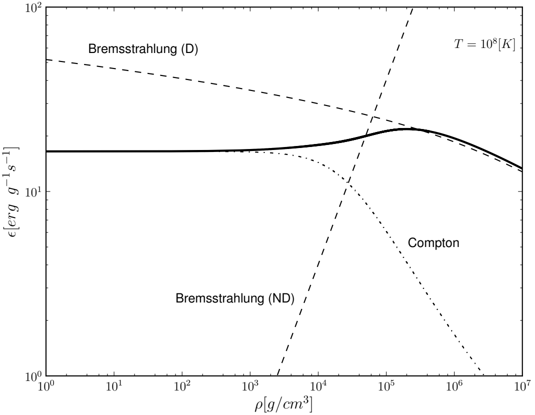

Figure: Different axion emission processes and the interpolated axion emissivity in continuous line

Along this work, we use the Princeton-Goddard-PUC (PGPUC; Valcarce et al. 2012) stellar evolution code.

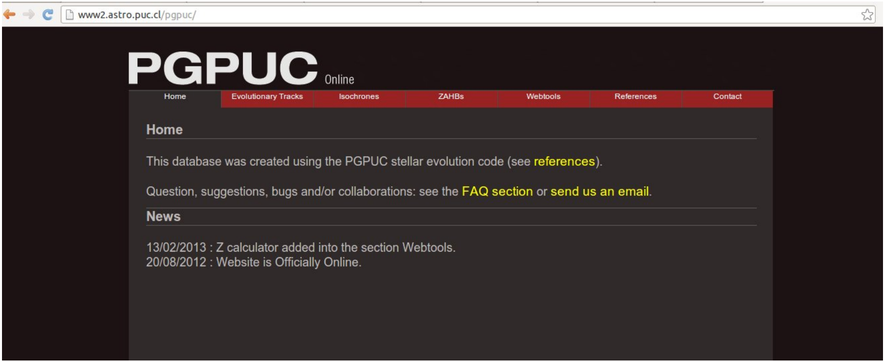

Tip of the RGB as test of novel effects

A sensitive observable to constrain enhanced energy losses is the brightness of the Tip of the RGB in GCs (Raffelt 1990, Raffelt & Weiss 1992, Catelan et al. 1996).

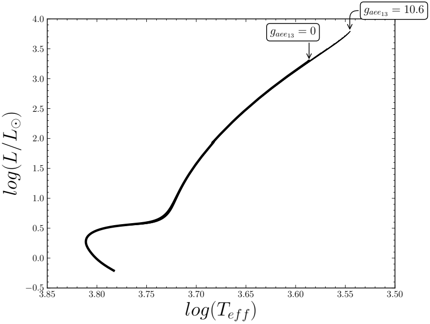

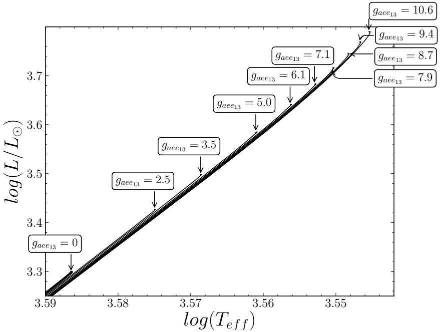

$g_{aee_{13}} = g_{aee} \times 10^{13}$

- Massive GC, with $M_V < -8.0$, to ensure well populated CMD.
- $E(B-V) < 0.1$, to reduce the possibility of differential reddening.
- Cluster metallicity not to high and not to low. Leading a uniformly populated HB.
- Avoid GCs where is strong evidence of multiple populations.

At the top of this selection, NGC5904 (M5) appears as a priority.

For M5, the data consist in 2840 CCD images, obtained during 40 runs on 12 telescopes over a span of 27 years.

The photometry was did it with DAOPHOT II/ALLFRAME suite of programs (Stetson 1987, Stetson 1994).

With the CMD of M5 we perform a statistical decontamination for field stars (Gallart et al. 2003).

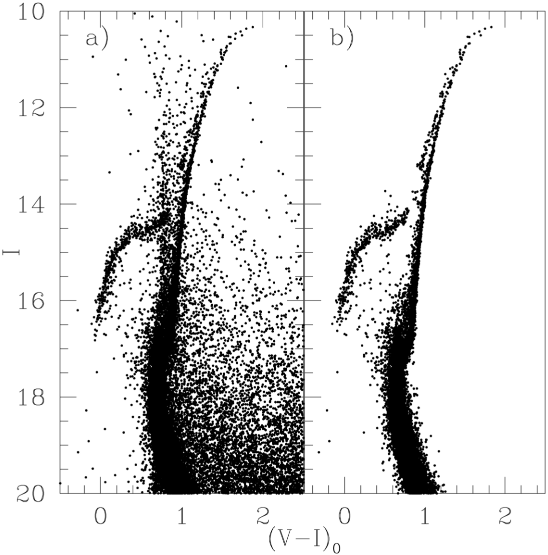
a)
b)
10
12
14
16
18
20
I
0
1
2
0
1
2
$(V-I)_0$

One of our main point of interest is the TRGB. But for Milky Way GCs the evolution of RGB near the TRGB is very fast and in the CMD this region is poorly populated. We need a statistical approach is needed.

Several methods are described in the literature (Bellazini et al. 2002, Makarov et al. 2006, Madore et al 2009), but these methods are aimed to resolve more populated populations near the TRGB as ω Centauri and resolved galaxies.

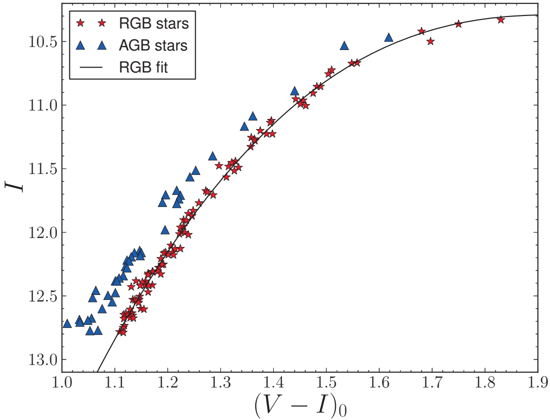

$$I = I_0 + 3.83[1.95 - (V - I)]^{2.5}$$

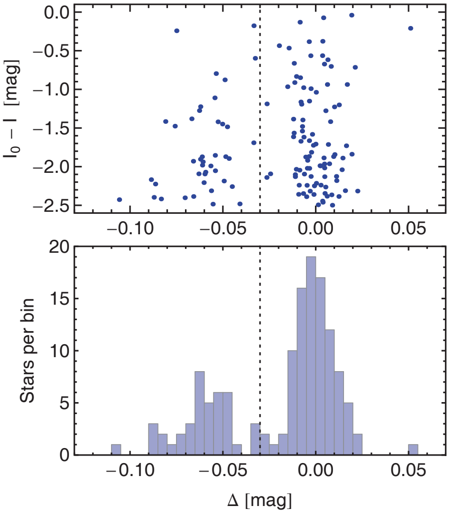
0.0
−0.5
−1.0
−1.5
−2.0
−2.5
$I_0 - I$ [mag]
−0.10
−0.05
0.00
0.05
20
15
10
5
0
Stars per bin
Δ [mag]

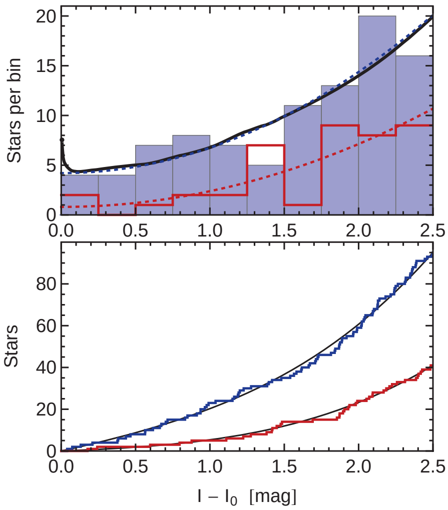

$$\frac{dN_{\mathrm{RGB}}}{dI} = N_{\mathrm{RGB}} \left[a + b\,(I - I_0)^2\right] , \qquad (10)$$

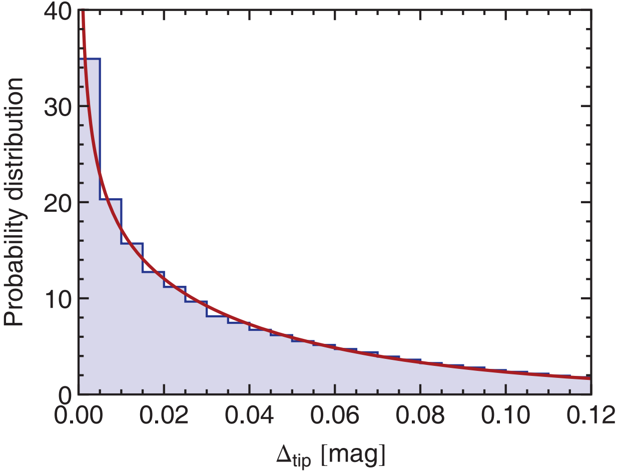

$$p(\Delta_{\rm tip}) = \frac{e^{-\Delta_{\rm tip}/\lambda}}{\lambda}\,\frac{1 + a\,\Delta_{\rm tip}^{-1/3}}{1 + a\,\lambda^{-1/3}\,\Gamma_{2/3}}\,, \qquad (11)$$

Tip of the RGB for M5

We conclude that the Tip of the RGB is within 0.05 mag at 68% C.L, and within 0.16 mag at 95% C.L

Summarizing observational uncertainties

The TRGB is located in the interval $M_{I,TRGB}^{obs} = -4.17 \pm 0.13$ mag
.
This is obtained summing in quadrature the individual error sources:

- TRGB 0.058 mag.
- Calibration of the photometry, ± 0.02 mag.
- Saturation, completeness and crowding, combined contribute less than ± 0.01 mag.
- Distance Modulus, ± 0.11 mag

Detailed discussion of each one you can find in Viaux et. al. 2013 I (Submitted to A&A)

Summarizing theoretical uncertainties

Table: Error budget in theoretically predicted $M_{I,\mathrm{TRGB}}^{\mathrm{the}}$

Input quantity	**Adopted Range**	$\mathbf{\Delta M_{I,TRGB}}$ **[0.01 mag]**
Mass ($M_\odot$)	0.820 ± 0.025	± 0.2
Y	0.245 ± 0.015	± 1.0
Z	0.00136 ± 0.00035	$+0.7/-0$
$[\alpha/\mathrm{Fe}]$	0.3 ± 0.1	∓ 0.4
α_{MLT}	$\alpha_{\mathrm{MLT}}^{\mathrm{calibrated}} \pm 0.2$	± 5.6
Atomic diffusion	See text	$+0/-0.6$
Boundary conditions	$(1 \pm 0.05)\, T(\tau)$	∓ 0.7
κ_{rad}	$\pm 10\%$	∓ 0.02
κ_{c}	$\pm 10\%$	± 1.6
Nuclear Rates	See Table 1, Viaux et al. 2013 I	± 1.9

Summarizing theoretical uncertainties

Table: Error budget in theoretically predicted $M_{I,\mathrm{TRGB}}^{\mathrm{the}}$

Input quantity	**Adopted Range**	$\mathbf{\Delta M_{I,TRGB}}$ **[0.01 mag]**
Neutrino emission	$\pm 5\%$	∓ 1.3
EOS	8 cases	$+2.4/-0.5$
Mass loss ($M_\odot$)	0.12–0.28	$+2.2/+3.5$

Comparing observational and theoretical results

For the theory, finally we have:

$$\begin{aligned} M_{I,\mathrm{TRGB}}^{\mathrm{theory}} &= -3.99 - 0.23 \left(\sqrt{g_{aee_{13}}^2 + 0.9^2} - 0.9 - 0.17\, g_{aee_{13}}^{1.5} \right) \\ &\quad \pm \sqrt{0.039^2 + (0.06 + 0.01 g_{aee_{13}})^2}. \end{aligned}$$

And:

$$M_{I,TRGB}^{obs} = -4.17 \pm 0.13$$

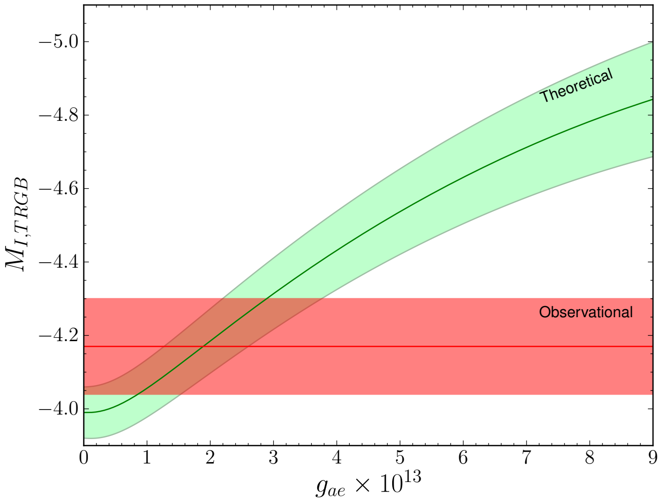
Theoretical
Observational
$M_{I,TRGB}$
−5.0
−4.8
−4.6
−4.4
−4.2
−4.0
0
1
2
3
4
5
6
7
8
9
$g_{ae} \times 10^{13}$

Finally integrating the combined probability distribution:

$$\begin{aligned} g_{aee} &< 2.7 \times 10^{-13} \quad \text{at } 68\% \text{ CL},(m_a \sim 9.6 meV) \\ g_{aee} &< 4.7 \times 10^{-13} \quad \text{at } 95\% \text{ CL}.(m_a \sim 16.8 meV) \end{aligned} \tag{12}$$

Table: Summary of the g_{aee} constraint

Authors	g_{aee}	$m_a \cos^2 \beta$	C.L.
Raffelt & Weiss 1995	$\lesssim 2.5 \times 10^{-13}$	$\lesssim 8.9$ meV	-
Catelan et al. 1996	$\lesssim 2.1 \times 10^{-13}$	$\lesssim 7.5$ meV	-
Isern et al. 2013	$\sim 2.2 \times 10^{-13}$	$\lesssim 7.9$ meV	-
Córsico et al. 2012	3.2×10^{-13}	$\lesssim 11.4$ meV	68%
Viaux et al. 2013 II			
(To be submitted)	$\lesssim 2.7 \times 10^{-13}$	$\lesssim 9.6$ meV	68%
	$\lesssim 4.7 \times 10^{-13}$	$\lesssim 16.8$ meV	95%

Viaux et al. 2013 I

$$\begin{aligned} \mu_\nu &< 2.6 \times 10^{-12} \mu_{\mathrm{B}} \quad \text{at 68\% CL,} \\ \mu_\nu &< 4.5 \times 10^{-12} \mu_{\mathrm{B}} \quad \text{at 95\% CL.} \end{aligned} \tag{13}$$

Versus,

$$\mu_{\bar{\nu}_e} < 3.2 \times 10^{-11}\, \mu_{\mathrm{B}} (90\%\ CL)$$

Beda et al. 2010.